Industrial Crops & Products 204 (2023) 117336

Contents lists available at ScienceDirect

Industrial Crops & Products

journal homepage: www.elsevier.com/locate/indcrop

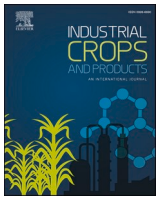

Harvesting value from agricultural waste: Dimensionally stable fiberboards and particleboards with enhanced mechanical performance and fire retardancy through the use of lignocellulosic nanofibers

Amira Najahi [a], Roberto J. Aguado [b], Quim Tarrés [b,*], Sami Boufi [a], Marc Delgado-Aguilar [b]

[a] University of Sfax - LMSE - Faculty of Science - BP 802, 3018 Sfax, Tunisia
[b] LEPAMAP-PRODIS Research Group, University of Girona, C/ Maria Aurèlia Capmany, 61, 17003 Girona, Spain

ARTICLE INFO

Keywords:
Lignocellulosic nanofibers
Particleboards
Fiberboards
Agricultural waste
Lignocellulosic materials

ABSTRACT

The present work provides a comprehensive study on the utilization of rapeseed stalks, an agricultural waste, as a raw material for the production of resin-free fiberboards and particleboards, using LCNFs as binder. The rapeseed stalks underwent appropriate crushing and fibrillation and were combined with a novel class of lignocellulosic nanofibers (LCNFs) derived from date palm waste, another agricultural residue. The incorporation of LCNFs in both fiberboards and particleboards resulted in increased density and enhanced mechanical properties, dimensional stability, and fire resistance. These positive effects can be attributed to several factors. Firstly, the incorporation of LCNFs led to a reduction in porosity, positively impacting the modulus of rupture, modulus of elasticity, and internal bonding of the produced fiberboards and particleboards. Notably, fiberboards containing 15 wt% LCNF exhibited superior specific properties compared to our commercial reference. Additionally, this densification effect mitigated moisture absorption and thickness swelling, as even a 2 wt% incorporation of LCNF in fiberboards showed reduced values for both properties. Secondly, the high lignin content of the LCNFs contributed to decreased hydrophilicity in the fiberboards and particleboards, leading to significant improvements in water contact angle, water absorption, and thickness swelling. Lastly, the increased density of the fiberboards and particleboards resulted in improved fire resistance, with flame propagation time being higher for all boards containing LCNFs, even at low content (2 wt%), compared to the commercial fiberboard. Notably, fiberboards demonstrated superior performance compared to particleboards, attributed to factors such as low cohesion, particle heterogeneity, and excessive porosity. Overall, this study demonstrates the feasibility of utilizing agricultural waste as a raw material for board production, eliminating the need for urea-formaldehyde resins and paraffin waxes commonly found in commercial fiberboards.

1. Introduction

The construction and building industry is currently one of the largest contributors to the economy and job creation (Shojaei et al., 2021), but it requires the use of a significant amount of natural resources, leading to negative environmental impacts (Buyle et al., 2013). In recent years, modular construction has gained popularity as a means of increasing automation and productivity in this traditionally non-industrialized sector. This approach involves the use of lighter and mass-produced materials and structures, such as wood-based boards (Aguilar et al., 2020; Gan et al., 2022).

Wood-based boards, commonly referred to as particleboard or high/medium density fiberboards (HDF and MDF, respectively), offer numerous advantages, including low cost, processability, smooth surface, and mass-production. However, these boards have certain drawbacks and limitations. They typically rely on synthetic resins, such as formaldehyde-based resins, for binding the particles or fibers, which raises health and safety concerns (Hashim et al., 2009). According to the World Health Organization, low exposure to formaldehyde can already cause eyes, nose, and throat irritation, and it is classified as a carcinogen. Long-term exposure can lead to chronic lung problems, dermatitis, allergic eczema, and cancer (Kim et al., 2011). In fact, some countries such as Sweden or Germany have already established a maximum permissible indoor formaldehyde concentration of 0.1 ppm (Schieweck

* Corresponding author.
E-mail address: joaquimagusti.tarres@udg.edu (Q. Tarrés).

https://doi.org/10.1016/j.indcrop.2023.117336
Received 3 July 2023; Received in revised form 11 August 2023; Accepted 15 August 2023
Available online 21 August 2023

et al., 2018). Additionally, they exhibit high affinity to water and moisture, limiting their outdoor applications, and have limited resistance to fire (Troilo et al., 2023).

To address these challenges, there is a growing emphasis on the development of safe and bio-based binders to optimize the performance of fiberboards produced from alternative fibers. Researchers have explored the incorporation of lignin into fiberboards as well as leveraging the inherent lignin present in the fibers by modifying the hot pressing process parameters (Domínguez-Robles et al., 2018; Zhang et al., 2015). Calcium lignosulfonate has also been investigated as a lignin-based additive, showing improved moisture absorption and mechanical properties (Antov et al., 2021). However, there is a limited number of works demonstrating the viability of lignin as a binder in urea-formaldehyde-free adhesive for wood panels (Mancera et al., 2012, 2011). The extensive use of virgin wood fibers across various industries has led to a significant strain on this resource, resulting in a shortage of raw materials and an associated increase in prices (Aguilar et al., 2020). By reducing reliance on virgin wood fibers through the implementation of more sustainable practices, such as the use of recycled or alternative materials, the pressure on this resource could be alleviated, ensuring its availability for future generations. Thus, the use of alternative fiber sources for fiberboard production, such as agricultural residues, is becoming a topic of great interest as it contributes to forest preservation while valorizing residues from the primary sector (Domínguez-Robles et al., 2020; Halvarsson et al., 2009; Nasir et al., 2019). Other sources encompass the use of recycled fibers, yet they exhibit lower performance and properties than virgin fibers (Antov et al., 2021; Ye et al., 2007). By incorporating alternative fiber sources and reducing the reliance on virgin wood fibers, the production of fiberboards can become more sustainable, addressing the strain on natural resources and promoting the preservation of forests for future generations.

Another approach to enhance the mechanical properties of fiberboards is the incorporation of cellulose nanofibers (CNFs) and lignocellulosic nanofibers (LCNFs). These nanofibers have been shown to significantly improve the strength and modulus of fiberboards (Kaffashsaei et al., 2023; Kojima et al., 2016; Theng et al., 2015). Although CNFs possess remarkable bonding capabilities, their hydrophilic nature limits their water resistance, preventing their use in outdoor applications (Arévalo and Peijs, 2016; Sehaqui et al., 2011).

Nanotechnology has emerged as a pivotal field, revolutionizing various industries through the integration of nanomaterials. Tozluoglu et al. (2022), and Zor et al. (2022) delve into the enhancement of paper and board coatings, as well as the augmentation of wood plastic composites, respectively, through the strategic incorporation of nanocellulose. By harnessing nanocellulose's unique properties, these investigations illustrate how material functionalities and qualities can be significantly bolstered. Building upon this foundation, Kocaturk et al. (2023) delve into the recent strides achieved in lignin-based biofuel production—an endeavor promising both sustainable energy sources and eco-friendly practices. Meanwhile, the works by Candan et al. (2022); Yildirim et al., (2022, 2021); Yildirim and Candan (2021) collectively underscore the transformative role of nanocellulose in the development of novel adhesives, composites, and particleboard panels. By incorporating nanocellulose and boron compounds, these studies demonstrate significant enhancements in material performance and properties.

Furthermore, Yildirim et al. (2021) explore the realm of hybrid resin systems, revealing the intricate chemistry behind the reinforcement of urea-formaldehyde resins with nanocellulose and boron compounds. This exploration, alongside the works of Candan et al. (2016), employing dynamic mechanical thermal analysis (DMTA) to unravel the viscoelastic behavior of nanocomposites, adds a deeper dimension to the understanding of these materials' characteristics.

Improving the fire resistance of medium density fiberboards (MDFs) has been a long-standing challenge. Traditionally, additives based on aluminum trihydroxide or poly-phosphates have been incorporated, but they can adversely affect fiber adhesion and require the use of urea-formaldehyde resins (Hashim et al., 2005; Mantanis et al., 2020). Exploring alternative methods, such as the incorporation of natural fire retardants, offers a more sustainable and cost-effective approach (Cheng et al., 2020; Ur Rehman et al., 2021).

In light of these considerations, this study aims to develop particleboards and fiberboards using rapeseed stalk, a significant agricultural residue from oil production, in conjunction with lignocellulosic nanofibers derived from date palm waste. The LCNFs will be used as binders in the range of 0–15 wt%, offering a sustainable solution while valorizing two globally relevant residues for value-added product manufacturing. By addressing the limitations of traditional wood-based boards and incorporating innovative binders and reinforcement materials, the present work aims to enhance the performance, water resistance, and fire resistance of the produced boards, contributing to the development of sustainable and high-performance building materials.

2. Experimental section

2.1. Materials

Rapeseed straw was kindly supplied by Mas Clarà S.L. (Domeny, Spain) and was used as raw material for manufacturing both particle- and fiberboards. Date palm waste was kindly supplied by farmers from the Gabès region (Gabès, Tunisia) during the annual pruning of date palm trees, and was used for the production of LCNFs. All the required reagents for the experimentation, including boards and LCNFs production and characterization, were acquired at Merck KGaA (Darmstadt, Germany). The commercial boards were purchased at the Leroy Merlin store in Girona (Girona, Spain).

2.2. Rapeseed particles and fibers preparation and characterization

Rapeseed straw was completely crushed using a knife mill from Agrimsa, equipped with a 5 mm sieve at the bottom. The resulting particles were either directly used for particleboard production or, on the other hand, subjected to mechanical fibrillation in a Sprout-Waldron refiner lubricated with cold water from Andritz (Graz, Austria). The resulting fibers were centrifuged to remove the excess of water and stored in hermetic plastic bags at 4 °C for further use and characterization.

Rapeseed particles (RP) and fibers (RF) were observed by means of optical microscopy (OM) using a LEICA DMR-XA optical microscope equipped with a camera NIKON F90 and RICOH X-RX3000. Fiber morphology was analyzed using a MorFi Compact Analyzer from Techpap (Grenoble, France) equipped with a CCD video camera able to analyze 30,000 fibers from a 25 mg/L suspension per test, aided by the MorFi software. Among other parameters, the software provides relevant morphological features such as length, diameter, ratio of macrofibrils or fines content.

The chemical composition of both particles and fibers was also analyzed. Ash content was determined through gravimetry, which involved combusting the sample in a furnace at 525 °C following the TAPPI T211 standard. The insoluble lignin content was measured through acid hydrolysis on a sample without extractives, following the TAPPI T222 standard. A sample of fibers (typically 300 mg) was taken and subjected to hydrolysis. Hydrolysis was carried out by adding 3 mL of 72 wt% H_2SO_4 (sulfuric acid) to the sample. The mixture was then allowed to react at a temperature of 30 °C for a duration of 1 h. After hydrolysis, deionized water was added to the sample, typically 84 g. The sample, along with the water, was then placed in an autoclave, and the sample was autoclaved at a temperature of 121 °C for a duration of 1 h. Once the hydrolysis and autoclaving steps were completed, the hydrolyzed sample was subjected to vacuum filtration. The sediment collected on the filter was then carefully dried and weighed. The weight of the sediment represents the Klason lignin content in the original sample.

Then, the hemicellulose content was determined through colorimetry after acid boiling, following the TAPPI T223 standard. This method involves reacting the hemicellulose with orcinol, in the presence of concentrated sulfuric acid. The resulting color intensity was measured using a spectrophotometer at a specific wavelength, often 660 nm. A calibration curve was used to correlate the color intensity to the hemicellulose concentration in the sample. Finally, the cellulose content was estimated through the difference method.

2.3. LCNF production and characterization

As indicated above, LCNFs were prepared from date palm waste (DPW). For this, DPW underwent a multiple-stage process encompassing biomass preparation, a chemical treatment with maleic acid, and fibrillation by means of high-pressure homogenization.

DPW was firstly crushed following the same procedure than the one described for rapeseed stalks. Then, the DPW particles were fibrillated in a Sprout-Waldron refiner using cold water as lubricant. As in the case of rapeseed stalks, the resulting fiber suspension was thoroughly centrifuged to remove the excess of water and stored in hermetic plastic bags at 4 °C for further use and characterization. These fibers were referred to as DPW. Then, fibers were subjected to a hydrothermal treatment (HT) in a stainless-steel reactor to further promote fiber individualization. Fibers were suspended in distilled water at a solid-to-liquid ratio of 1:10. The suspension was heated to 160 °C for 3 h and 30 min under gentle stirring. These fibers were referred to as DPW-HT. After the hydrothermal treatment, fibers were treated with 20% maleic acid solution. The reaction was carried out in the same reactor, but temperature was set at 150 °C for 2 h. The maleic acid treated fibers were thoroughly washed with distilled water to eliminate excess of acid and then with a sodium hydroxide solution to maintain the pH around 8. The resulting fibers from this treatment, were referred to as DPW-HT-MA.

The treated fiber suspension, with a solid content of approximately 1.5 wt%, underwent a three-pass high-pressure homogenization process using a GEA Niro Soavi (NS1001L PANDA 2 K-GEA, Italy) at a pressure of around 300 bar, followed by three additional passes at 600 bar.

The resulting fibers (DPW, DPW-HT, and DPW-HT-MA) were characterized in terms of chemical composition, following the above-described protocol, and observed by optical microscopy using the same equipment and conditions than for rapeseed particles and fibers. The DPW, DPW-HT, and DPW-HT-MA were also characterized in terms of morphology using the MorFi equipment. AFM images were obtained using a multimode scanning probe microscope setup driven by the Nanoscope IIIa electronics (Digital Instruments, New York, USA) in the intermittent contact mode at room conditions. The determination of the degree of polymerization (DP) followed the standard cellulose measurement method, TAPPI T236. In this procedure, dried fibers (ranging from 0.15 to 0.05 g) were dissolved in 0.5 M copper ethylenediamine (CED) solution (20 mL). The intrinsic viscosities of these solutions were measured using a Cannon-Fenske capillary viscometer. The DP was subsequently calculated using the Mark-Houwink-Sakurada equation, with a power-law exponent of 0.905: $DP = 0.75\ [\eta]$.

Achieving complete dissolution of the fibers required a dissolution time of 1–2 days. However, for unmodified DPW (dissolving pulp) and fibers containing lignin exceeding 15 wt%, an additional delignification step was necessary. This delignification process involved using sodium chlorite (NaClO2), a selective delignifying agent that doesn't degrade the fibers. Specifically, for this step, 0.6 g of NaClO2 and 1 mL of glacial CH3COOH were added per gram of fiber. Prior to delignification, the fibers were dispersed in 50 mL of water. The resulting suspension was then stirred at 70 °C for 1 h until the fibers turned white and achieved complete individualization.

2.4. Fiberboard and particleboard production and characterization

Both particle- and fiberboards were prepared by means of a wet process, encompassing particle or fiber suspension and cake formation to achieve an appropriate mass distribution along the surface of the board. Both for the case of boards made of particles and made of fibers, rapeseed was suspended in water at 5 wt% consistency and subjected to disintegration in a laboratory pulper for 20 min at 1100 rpm. The LCNF dosage ranged from 0 to 15 wt% and were incorporated into the pulper together with the particles or the fibers. The resulting suspension was then subjected to gentle stirring in presence of 0.5 wt% of cationic starch as retention agent. In order to form a uniform cake, a home-made Rapid-Köthen-like filtration column was used. The amount of suspension was calculated to obtain a circular cake with a dry basis weight accounting for 3 kg/m^2. The cake was sliced into samples of 175 × 75 mm^2 and introduced into a stainless-steel mold of the same size. The wet sample, together with the mold, was introduced into a hot press machine Lab-Econ 300 from Fontijne Grotnes B.V. (Vlaardingen, Netherlands).

Hot-pressing was performed by multiple stages modifying both pressure and temperature. First of all, the sample was subjected to a pressure of 8 MPa at 75 °C for three minutes. Then, the pressure was released to be immediately increased to 14 MPa. Pressure cycles allow the release of water vapor from the wet cake, promoting fiber compaction and interactions. After 5 min at 14 MPa and 75 °C, temperature was raised to 150 °C and pressure, decreased to 8 MPa. These conditions were maintained for 60 min. The temperature was then gradually increased to 230 °C, above lignin's Tg, and the pressure increased again to 14 MPa. Finally, the board was gradually decompressed and pressed again for 5 min at 230 °C and 14 MPa. With these conditions, the resulting boards exhibited a thickness of around 3 mm. Boards were then cut into 175 × 25 mm^2 specimens and conditioned in a climatic chamber from Dycometal (Viladecans, Spain) at 50% of relative humidity and 23 °C for 48 h, before physic and mechanical characterization.

The characterization of the boards consisted of several physical features, including dimensional stability and their behavior against water and moisture, and mechanical properties, namely modulus of rupture (MOR) and elasticity (MOE), and internal bonding (IB). Further, the fire resistance of the obtained boards was assessed.

The thickness of all the boards was determined in a dead-weight micrometer (Starrett, Athol, USA), taking 10 measurements from randomly selected points of the board surface and expressed as the average of these measurements. Considering the dimensions of the boards and their weight, density was easily calculated by referring the board weight to its volume, expressing the values in kg/m^3. The dimensional stability of the boards was assessed by means of two different parameters, namely water absorption and thickness swelling. Water absorption was determined according to the UNE-EN 317:1993 standard and thickness swelling according to UNE-EN 382:1992. Briefly, previously to analysis, the samples of 50 mm * 50 mm were conditioned in a controlled environment at 23 °C of temperature and 50% of relative humidity to ensure equilibrium moisture content. Then the samples were immersed in water for 72 h. The thickness and weight of the samples were determined to compare the post-immersion thickness with the initial thickness (thickness swelling) and the weight gain due to water absorption. The water contact angle of the boards was determined in a drop shape analyzer DSSA25 from Krüss GmbH (Hamburg, Germany), aided by the Krüss Advance software. The sampling frequency was set at 2 s^{-1} and results were expressed as the average of the WCA (left and right) as function of time. The total testing time was set at 180 s

MOR, MOE and IB were determined in a Universal Testing Machine Instron 1122. MOR and MOE were determined according to UNE-EN 310:1994, while IB was determined according to UNE-EN- 319:1994. Finally, fire resistance was determined according to UL94 Horizontal Burning Test standard, using specimens of 125 mm in length and 13 mm in width fixed horizontally from one of the ends. First of all, a 45° flame was placed at the free end of the specimen for 30 s. The specimen was marked at 25 and 100 mm, and the time that the flame took between these two points was recorded. The structure of the boards and their morphology in the cut section was observed by scanning electron

microscopy on a Zeiss DSM 960 A with a Silicon drift droplet detector (SD3) (Oberkochen, Germany).

3. Results and discussion

3.1. Rapeseed particles and fibers characterization

Rapeseed stalks were collected from the field after harvesting, without any sorting, and taking advantage that stalks must be collected before the next planting season. These stalks, which are constituted by a cellulose-rich external part and the pith (Fig. S1). The latter represents roughly the 13% of the stalks by weight and negatively influences the yield of fiber extraction processes (Hýsek et al., 2018; Tofanica et al., 2011). However, aiming at preserving the maximum residue, the pith was not removed from the stalks before processing.

Rapeseed stalks exhibit a heterogeneous structure, even more than wood species, as they contain parenchyma and tracheid cells, vessel elements and lignocellulosic fibers, composed by cellulose, hemicellulose and lignin (Tofanica et al., 2011). These lignocellulosic fibers, shown in Fig. 1a, are of great interest for fiberboard production, mainly due to their chemical composition and morphology. Due to the absence of any thermal or chemical treatment prior fibrillation, the fibers randomly broke down into smaller particles, leading to irregularities on fiber morphology, extensive external fibrillation, and the generation of finer elements released from the main fibers. Indeed, as revealed in Fig. 1a, some fibers with lengths above 1500 μm were found, as well as several fiber bundles and particles. Fig. 1b provides the fiber length distribution of the rapeseed fibers.

The morphological analysis of the rapeseed fibers indicated that the average arithmetic length accounted for 173 μm and the average diameter, for 21.7 μm. This apparently differs from the optical microscopy observation. However, as revealed in Fig. 1b, the equipment already identified some objects in the range of 771–1075 μm, and 1075 to 1500 μm, which is in agreement with the fibers shown in Fig. 1a. Considering the average values, the slenderness ratio accounted for 8, which is significantly lower than previously reported values for rapeseed fibers (Mazhari Mousavi et al., 2013; Tsalagkas et al., 2021). Slenderness, or aspect ratio, contributes to the generation of an entangled network within the fiberboard structure, which may have a direct influence on the resulting mechanical properties. In this case, the calculated aspect ratio would indicate low entanglement capacity but, as observed in Fig. 1a, the presence of some long and slender fibers can contribute to the generation of a compact structure, promoting the interactions between fibers (Theng et al., 2017).

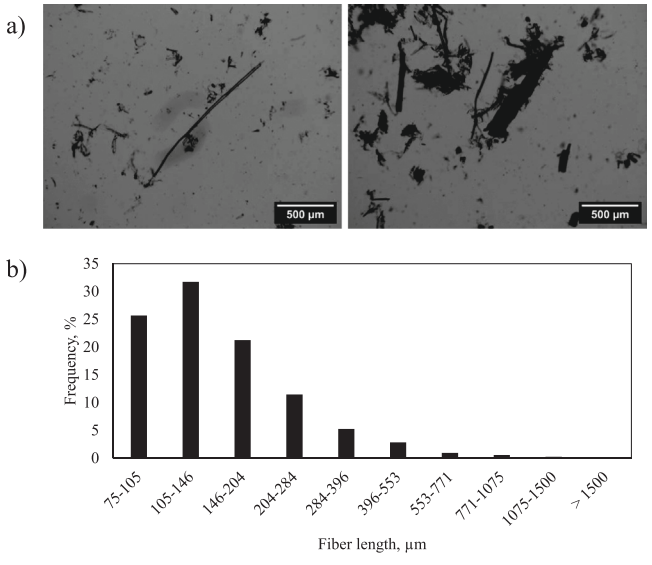

Fig. 1. Optical microscopy images of rapeseed fibers (a), and their fiber length distribution (b).

The chemical composition of the raw rapeseed stalks revealed a high cellulose content (50.6 wt%), a moderate hemicellulose content (23.8 wt%), and a lignin content of 19.8 wt%. The presence of ash was significant, accounting for 5.8 wt%. As expected, the fibrillation of rapeseed particles for obtaining fibers did not significantly affect the chemical composition, experiencing a slight decrease on the ash content (4.9 wt%), mainly due to the use of cold water for lubrication during fibrillation, and in the lignin content (19.3 wt%). According to Hýsek et al. (2018) and Tsalagkas et al. (2021), rapeseed exhibits cellulose and lignin contents in the range of 40 – 45 and 16 – 22 wt%, respectively, which are in agreement with the obtained results in the present study.

3.2. Date palm LCNFs characterization

Fig. 2 shows the chemical composition of the DPW as the different stages of the pretreatment, this is prior fibrillation, took place. Concretely, the chemical composition of the starting material (DPW), the DPW fibers after the hydrothermal treatment (DPW-HT), and the MA-treated fibers (DPW-HT-MA) is provided.

Comparatively to rapeseed, DPW exhibited a lower holocellulose content, with a significantly lower cellulose content and a slightly higher hemicellulose content. However, a significant difference came from the lignin, as in the case of DPW it accounted for 32 wt%. After the hydrothermal treatment, the main changes occurred in the hemicellulose and ash content. This was attributed to the removal of ash in hot water, as well as the partial solubilization of some hemicelluloses at high temperature (Herrera et al., 2014). Interestingly, lignin was preserved during this stage.

The subsequent treatment with maleic acid significantly increased the cellulose content from 42.0 to 59.5 wt%, while ash, lignin, and hemicellulose were partially removed. Notably, lignin content decreased from 31 to 21 wt%, which was attributed to the easier accessibility of maleic acid to amorphous regions. As it will be later discussed, this lignin removal was attributed to the partial dissolution of lignin, while its release in the form of nanoparticles (NPs).

Apart from the chemical changes, both the HT and the MA treatment had a direct influence over fiber morphology, as revealed by the optical microscopy images from Figs. 3a, 3b, and 3c. Fig. 3d shows an optical microscopy image of the obtained LCNFs from the DPW-HT-MA fibers.

The optical microscopy images clearly demonstrate notable alterations in fiber morphology following each treatment. For instance, the utilization of the Sprout-Waldron refiner (DPW) (Fig. 3a) resulted in the production of highly fibrillated and large fibers, which were subsequently fragmented into smaller fibrils. Analysis conducted with MorFi equipment indicated that the average fiber length was 326 μm, with an average diameter of 26.4 μm. Subsequent hydrothermal treatment, referred to as DPW-HT (Fig. 3b), caused further breakage of these larger

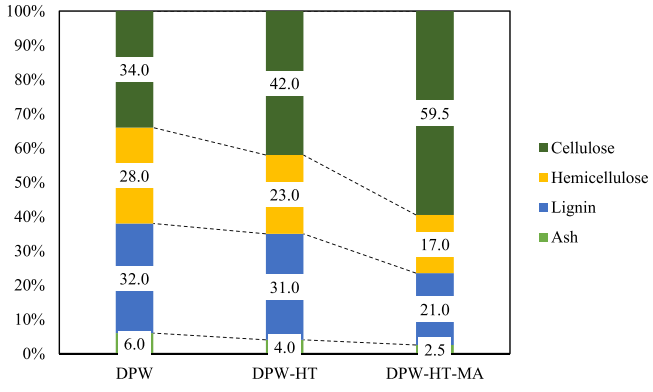

Fig. 2. Chemical composition of DPW, DPW-HT, and DPW-HT-MA.

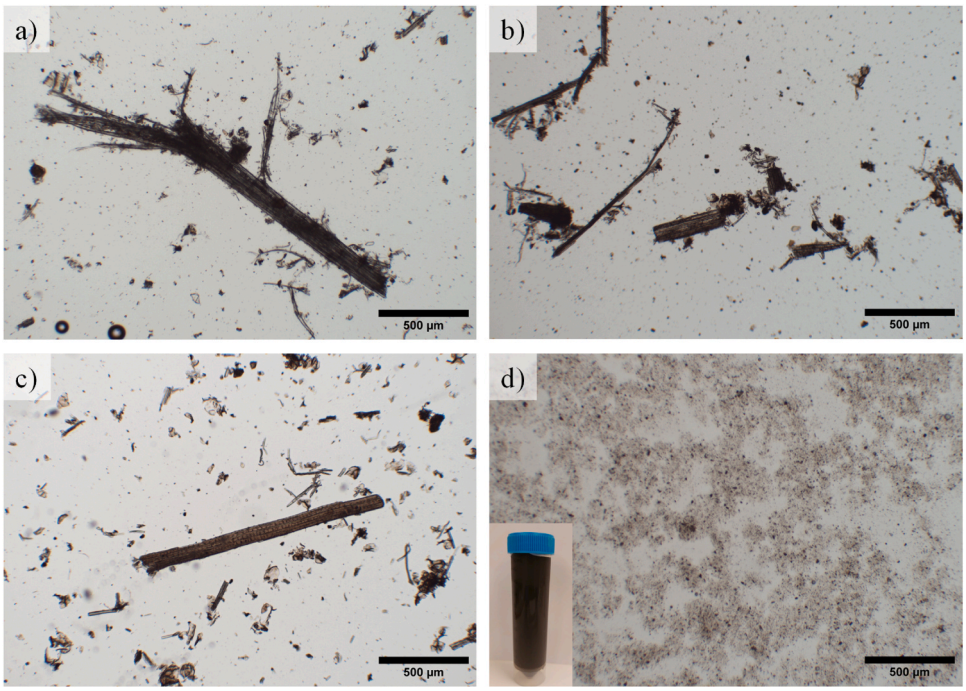

Fig. 3. Optical microscopy images of DPW (a), DPW-HT (b), DPW-HT-MA (c), and LCNFs (d). Inset image in (d) corresponds to a LCNF gel at 1.5 wt% consistency.

fibers, resulting in shorter fiber bundles and the release of smaller fibrils. This outcome is consistent with the morphological features obtained from MorFi analysis, where the average length and diameter were measured at 289 µm and 26 µm, respectively.

Although Fig. 3c reveals the presence of remaining long and thick fibers, it is evident that the action of maleic acid facilitated additional fibrillation. In fact, the average length decreased by 45% compared to the untreated DPW fibers, measuring at 178 µm, while the diameter accounted for 24.3 µm. Lastly, Fig. 3d presents an optical microscope image of the LCNF suspension. Although it does not provide specific information due to the unsuitability of this technique for nanosized objects, it does convey the significant reduction in fibril size when compared to the original untreated or treated fibers. However, the inset image reveals that passing a MA-treated suspension of DPW at a consistency of 1.5 wt% through the high-pressure homogenizer resulted in the formation of a thick and strong gel, which was stable even after 6 months without any sign neither of aggregation, nor phase separation.

Additional details regarding the characteristics of the obtained LCNFs can be found in the Supplementary Material (Fig. S2), as a separate study on LCNF production from DPW through MA treatment is currently being considered. Notably, the degree of polymerization (DP) of the initial DPW was measured at 2550, which experienced a significant decrease after the hydrothermal treatment (1551) and was further affected by the MA treatment, reaching a value of 223. Moreover, when the suspension was subjected to high-pressure homogenization, the LCNFs exhibited a DP of 197. This trend aligns with the observed reduction in fiber length throughout the various treatments, as supported by morphological analysis and previous studies on LCNFs and CNFs derived from different sources and processed through various methods (Shinoda et al., 2012; Tarrés et al., 2017).

Simultaneously, the relatively high temperature and the presence of MA promoted the chemical breakdown of the lignocellulosic constituents (lignin, hemicellulose, and cellulose), as evidenced by the significant decline in DP. This weakening of fiber cohesion facilitated the disintegration of the biomass into its elementary constituents during the mechanical action of high-pressure homogenization, as it will be later discussed. In fact, the cationic demand (CD) of the obtained LCNFs accounted for 372.8 µeq/g, which is remarkably higher than that of other CNF and LCNF species obtained through conventional treatments such as enzymatic hydrolysis or mechanical fibrillation (Serra-Parareda et al., 2021; Tarrés et al., 2016). This finding is consistent with the high water retention capacity of the LCNFs, which gradually increased with successive treatments of DPW. For instance, as shown in Table S1, the water retention value (WRV) increased from 1.25 g of H_2O per gram of fiber for the untreated DPW pulp to 3.83 g/g for DPW-HT-MA. Indeed, a reduction in both length and diameter is expected when fibers are exposed to shear forces within the pressure chambers of the high-pressure homogenizer, as depicted in Fig. 4 and Fig. S2, where diameters around 20 nm were observed. In addition, under the combined effect of pressure, temperature, and MA, the accessibility of the fiber to water and chemicals increases, favoring the expansion of the fibers and diffusion of water inside the fiber micropores. The above-mentioned breakdown of the lignocellulosic constituents, which weakens fiber cohesion, was found to generate individual nanosized fibrils, but also other nanosized particles that are hypothesized to be lignin nanoparticles (Fig. 4), as also found in previous works (Fontes et al., 2021; Hamawand et al., 2020).

The height profile analysis (Fig. 4b) indicated that the width of the fibrils was consistently below 4 nm, suggesting the presence of elementary cellulose fibrils. Additionally, the spherical nanoparticles (NPs) exhibited sizes ranging from 5 to 30 nm, and their surfaces did not appear flat, as evidenced by the similarity between their measured sizes and lateral dimensions in the high-resolution images. However, it is important to note that the AFM observations focused solely on the nanoscale fraction that remained in the supernatant after centrifugation, excluding the microsized fraction.

3.3. Fiberboards and particleboards using LCNF as a binder

As reflected in Fig. S3, as the LCNF content was increased on both particle- and fiberboards, their appearance became more brownish due to the increasing fraction of LCNF and, thus, the incorporation of a lignin-rich fraction. Moreover, this brownish surface can be also attributed to the diffusion of lignin, as the working temperature at the hot press was set above the softening temperature of lignin.

The density of particle- and fiberboads is a crucial factor that

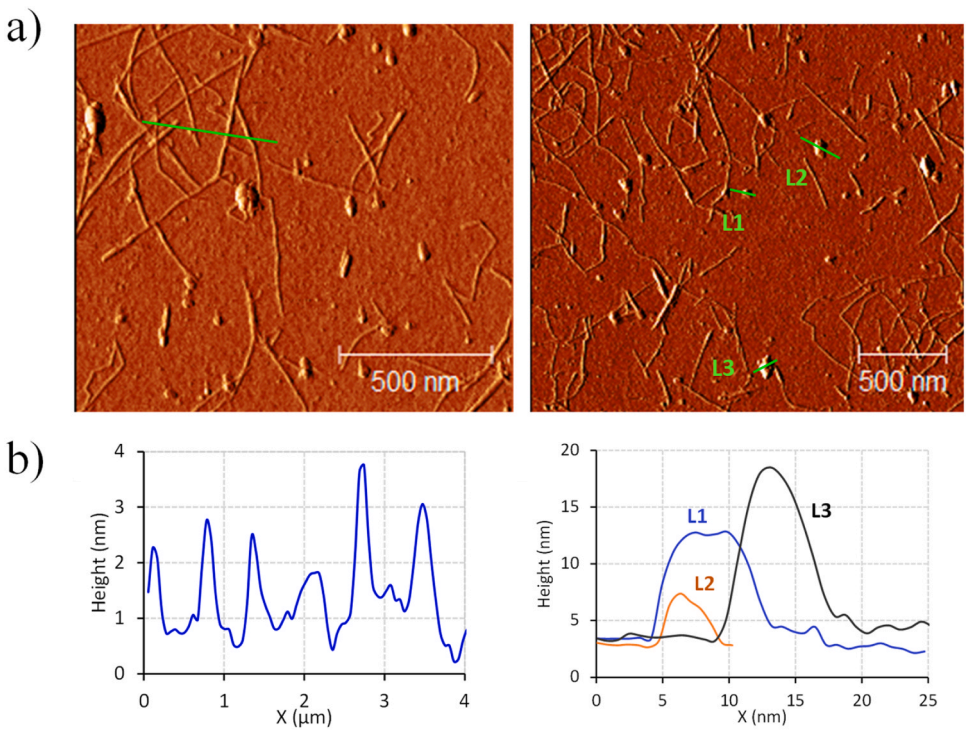

Fig. 4. AFM images of LCNFs (a) and the height profile analysis of the green marks on AFM images (b).

significantly impacts their properties. Medium-density fiberboards (MDF) typically fall within the range of 500–800 kg/m^3, whereas boards with higher densities are classified as hardboards (Nourbakhsh et al., 2010). At a constant basis weight, thickness directly correlates with density. In this study, the density and thickness of the manufactured fiberboards and particleboards were compared to those of a reference commercial fiberboard, which presented a density of 850 kg/m^3 and a thickness of 3 mm. Fig. 5 shows the evolution of particle- and fiberboards density as function of the LCNF content, compared to the commercial reference and those boards without LCNFs.

In comparison, the neat particleboard (0 wt% LCNF) exhibited the lowest density among the tested samples. This can be attributed to the larger size of the particles comprising the board and their lower bonding capacity due to the reduced surface area. When 5 wt% of LCNF was incorporated into the particleboard, the density increased by 27%, reaching a density similar to that of the commercial fiberboard. Furthermore, with an increased LCNF dosage of 10 wt%, a density of 993 kg/m^3 was achieved, nearly approaching the density of the neat fiberboard made from rapeseed fibers (1050 kg/m^3). Although this density was slightly higher than that reported in previous studies using

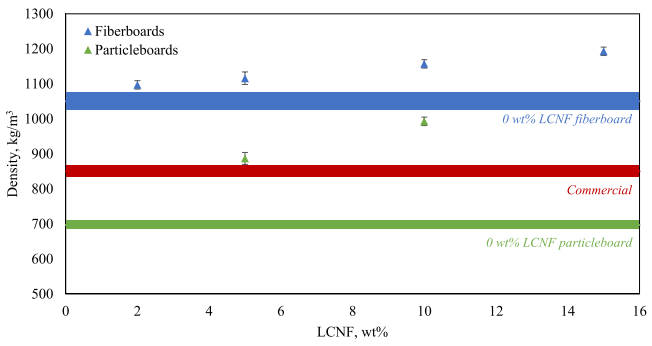

Fig. 5. Evolution of density with the LCNF content for particle- and fiberboards. Shadow areas represent the standard deviation of the 0 wt% LCNF particle- and fiberboard, and the commercial reference.

thermomechanical fibers from corn stalks, it can be attributed to slight differences in the pressing conditions (Theng et al., 2015).

In contrast, the obtained boards demonstrated lower density compared to rice fibers extracted through extrusion (1273–1390 kg/m^3), indicating that both the raw material and the processing methods can influence the compaction of fiberboards (Theng et al., 2019). The superior density of the obtained fiberboards can be attributed to the bonding mechanism in resin-free structures, primarily driven by hydrogen bonding, electrostatic interactions, and lignin softening and binding, particularly when the wet process is selected for fiberboard production, as it is comparable to papermaking (Page, 1969). Further, at the time of hot pressing, reactions such as dehydration, hydrolysis, and oxidation have been reported. Actually, hemicelluloses are believed to be decomposed first into organic acids, acetone, and furfural, followed by lignin and cellulose (Okuda et al., 2006; Rowell and McSweeny, 2008; Xu et al., 2003). In comparison, commercial fiberboards rely on synthetic resins to bind all the fibers and particles together, limiting natural interactions between the lignocellulosic constituents. Furthermore, rapeseed fibers are smaller in size than the wood fibers commonly used in the board industry, which typically range from 2 to 5 mm, resulting in lower compaction capacity (Li et al., 2009).

The incorporation of LCNFs into rapeseed fibers for fiberboard production resulted in density increases of 4.47%, 6.29%, 10.19%, and 13.62% for LCNF additions of 2 wt%, 5 wt%, 10 wt%, and 15 wt%, respectively. These density values represent 1.29, 1.31, 1.36, and 1.40 times the density of the commercial reference, respectively. In this case, beyond the abovementioned reaction mechanisms, the influence of shrinkage forces imparted by LCNFs within the board structure, together with an accentuated dehydration mechanism and the high surface area of nanosized lignocellulosic structures, are assumed as the main effects taking place on the improvement of board density (Theng et al., 2015; Thomas et al., 2018).

Figs. 6a and 6b present the water contact angle (WCA) evolution of fiberboards and particleboards, respectively, in comparison to the commercial reference. The commercial fiberboard demonstrated greater water repellency compared to the neat rapeseed fiberboards, particleboards, and fiberboards containing 2 wt% of LCNF. At equilibrium,

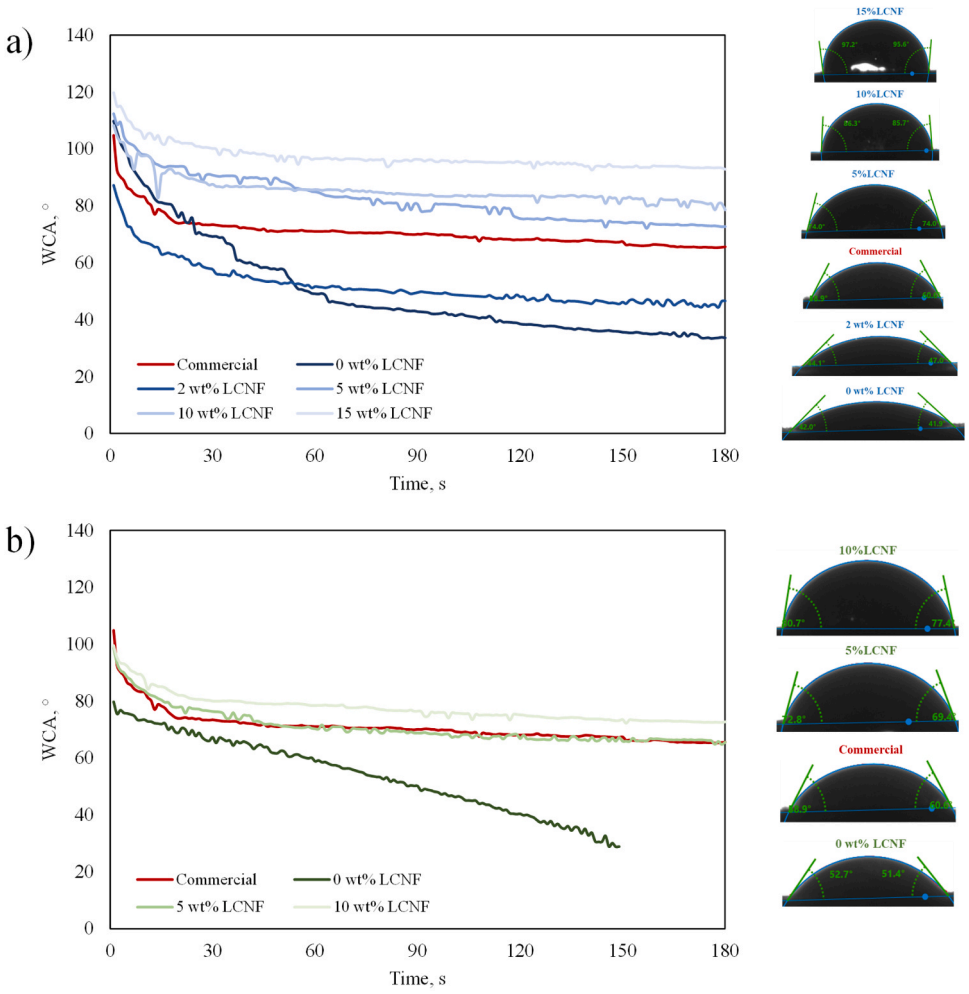

Fig. 6. Evolution of WCA and photo of a water drop at equilibrium of fiberboards (a) and particleboards (b).

when no significant changes in WCA were observed, the commercial fiberboard exhibited a WCA of approximately 60°, indicating a certain level of water repellency. This could be attributed to the intentional incorporation of paraffin waxes and UF resin, aimed at reducing hydrophilicity and improving board cohesion, respectively (Dunky and Niemz, 2002).

The higher WCAs observed when LCNFs were incorporated into both particleboards and fiberboards indicate the beneficial effects of this nanosized material in terms of dimensional stability and water protection. The decrease in hydrophilicity in both types of boards can be attributed to a combined effect of board cohesion and the presence of a high-lignin content constituent. Firstly, the incorporation of LCNFs, which are rich in lignin, along with the presence of lignin nanoparticles in the suspension, creates a barrier against water due to the hydrophobic nature of lignin. Fiberboards containing 15 wt% of LCNFs, in particular, exhibited a hydrophobic behavior with a WCA greater than 90°. Secondly, the shrinkage forces generated by LCNFs within the board lead to a compaction effect, reducing the porosity and thereby limiting water absorption by capillarity. This phenomenon has been previously reported when LCNFs were used for nanopaper making (Li et al., 2022; Najahi et al., 2023; Rojo et al., 2015). Thus, the improved WCAs observed when LCNFs are incorporated into particleboards and fiberboards can be attributed to the hydrophobic properties of lignin and the compaction effect resulting from the presence of LCNFs within the board structure. These factors contribute to enhanced dimensional stability and protection against water. This phenomenon becomes evident when contrasting the findings of Theng et al. (2015), wherein the utilization of nanofibers sourced from bleached pulp resulted in a notably lesser reduction in water absorption (minimum of 50%).

The dimensional stability of boards is usually assessed by means of the water absorption and thickness swelling. These measurements provide a comprehensive elucidation of their potential use for outdoor applications. Fig. 7 provides the evolution of both water absorption (WA) and thickness swelling (TS) for the obtained fiberboards and particleboards.

In the case of particleboards, the addition of 10 wt% LCNF was necessary to achieve a lower water absorption compared to the commercial fiberboard. The neat particleboard demonstrated a water absorption of 143% at the steady state, which was twice the value of the commercial fiberboard (70%). Although the incorporation of 5 wt% LCNFs reduced the water absorption to 83%, representing a decrease of 42%, the water absorption capacity remained higher than that of the commercial board. This observation can be strongly correlated with the particleboard density and the water contact angle (WCA), as similar values were found in both cases between the 5 wt% reinforced particleboard and the commercial reference. Similarly, the thickness swelling (TS) measurements indicated that none of the particleboards exhibited greater dimensional stability than the commercial board, as the TS value was noticeably higher in all cases, regardless of the LCNF content. However, it is worth noting that the particleboard containing 5 wt% of LCNFs exhibited remarkably higher TS, primarily due to increased accessibility through the edges of the particleboard. These findings suggest that while the incorporation of LCNFs improved water absorption and thickness swelling compared to the neat particleboard, it was

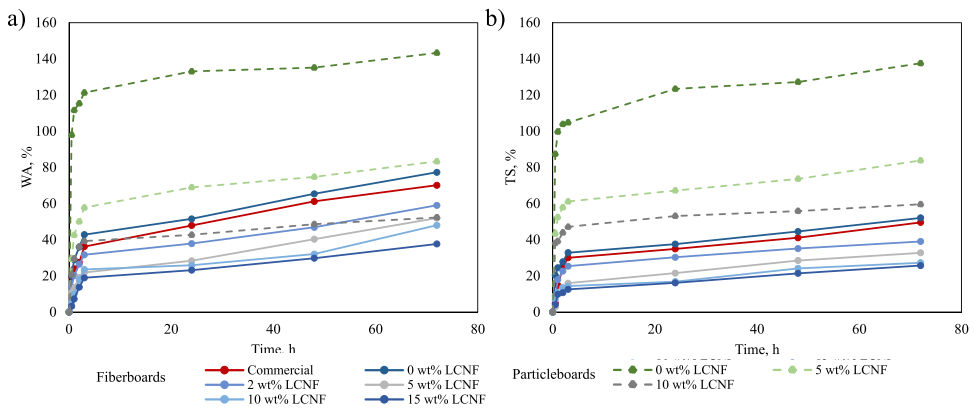

Fig. 7. Water absorption (a) and thickness swelling (b) of the obtained fiberboards and particleboards compared to the commercial reference.

still challenging to achieve performance on par with the commercial fiberboard. The particleboard density, water contact angle, and accessibility through the board's edges all played a role in determining the water absorption, thickness swelling and, thus, dimensional stability.

In contrast to particleboards, fiberboards demonstrated excellent performance in terms of water absorption and thickness swelling. The neat fiberboard exhibited dimensional stability comparable to the commercial reference, with slightly higher values of WA and TS. However, the addition of 2 wt% of LCNFs resulted in lower WA and TS values, which further decreased with increasing LCNF content. These findings align with the results obtained for contact angle, where the presence of LCNFs contributed to reducing the hydrophilicity of fiberboards, thereby limiting water diffusion through the fibrous structure. Additionally, the inclusion of LCNFs led to board densification, increasing surface tension and creating steric impediments to water.

These results are noteworthy, considering that some literature reports water absorptions of 100% in only 2 h (Diop et al., 2017). Interestingly, the incorporation of 15 wt% of LCNFs resulted in approximately half the WA and TS values of the commercial reference, accounting for 38% and 26% respectively. However, the inclusion of 10 wt% of LCNFs already had a significant effect on TS, indicating that the capacity of LCNFs to decrease hydrophilicity is limited. On one hand, LCNFs are hydrophilic, although they do possess some hydrophobic regions due to the presence of lignin (Rojo et al., 2015). On the other hand, the densifying capacity of LCNFs also has its limits (Liu et al., 2022; Sreejaya et al., 2022). Notably, the obtained results for TS are comparable to previously published findings where chitosan was used to improve water resistance and dimensional stability (Ji et al., 2017). Beyond the innocuousness brought by LCNFs when substituted to conventional urea-formaldehyde resins widely used as a binder in fiberboards, the remarkable enhancement in hydrophobicity of the material and reduction in water absorption constitute one of the main advantages to considering LCNFs as a potential binder in fiberboard and particleboard manufacturing. Indeed, due to the release of formaldehyde from fiberboard and the severe toxicity of formaldehyde, there is an urgent need to substitute urea-formaldehyde binder with a safer adhesive. In this sense, the use of biobased material will be of great benefit. The incorporation of LCNFs resulted in improved mechanical properties for both fiberboards and particleboards, as shown in Table 1. Specifically, the MOR of fiberboards exhibited a two-fold increase with a 15 wt% LCNF content. The neat and 2 wt% LCNF fiberboards demonstrated lower MOR and MOE compared to the commercial reference, while IB was higher for all the rapeseed fiberboards. Only fiberboards with a content higher than 5 wt% LCNF displayed greater MOR and MOE than the commercial board. However, when considering both MOR and MOE in relation to density, which normalizes the mechanical properties, it was found that only the fiberboard containing a 15 wt% LCNF exhibited superior mechanical performance compared to the commercial fiberboard. These findings align with previous studies using corn fibers and TEMPO-oxidized cellulose nanofibers (Theng et al., 2015). It is worth noting that while some authors have reported no significant improvements with the addition of LCNFs in fiberboards, the obtained results present a promising strategy for replacing UF resins in fiberboard production (Diop et al., 2017; Kojima et al., 2016). In relative terms, the inclusion of LCNFs in particleboards was found to be even more beneficial than in fiberboards, although none of the formulations achieved better mechanical performance than the commercial reference. Once again, this can be attributed to the lack of cohesion between particles, as well as the presence of bundles that hinder the full mechanical performance of rapeseed fibers. Nonetheless, the obtained results are higher than those reported in the literature for particleboards, which can be mainly attributed to the strong interactions between rapeseed particles and LCNFs from MA-treated DPW (Kojima et al., 2019).

The significant increase in mechanical properties can be attributed to the unique composition and morphology of the LCNFs, which consist of lignin nanoparticles and cellulose fibrils. Lignin contributed to adhesive, cohesive, and reduced hydrophilicity effects, while the cellulose fibrils primarily provided a reinforcing effect, enhancing the cohesion and internal bonding of the composite due to their intrinsic mechanical properties, and reducing the porosity. The addition of LCNFs improved

Table 1
Mechanical properties of the obtained fiberboards and particleboards.

	LCNF (wt%)	MOR (MPa)	MOE (GPa)	Specific MOR (MPa·cm^3/g)	Specific MOE (GPa·cm^3/g)	IB (MPa)
Commercial Fiberboard	0	48.59 ± 1.13^a	6.89 ± 0.31^a	57.16	8.11	0.89 ± 0.10^a
	0	39.35 ± 1.61^b	5.62 ± 0.26^b	37.48	5.35	1.18 ± 0.11^b
	2	46.12 ± 2.30^a	6.13 ± 0.29^b	42.04	5.59	1.26 ± 0.12^b
	5	52.99 ± 1.87^c	7.98 ± 0.29^c	47.48	7.15	1.39 ± 0.12^b
	10	62.47 ± 2.25^d	8.69 ± 0.37^c	53.99	7.51	1.48 ± 0.13^b
	15	76.13 ± 2.05^e	10.58 ± 0.32^d	63.81	8.87	1.71 ± 0.26^b
Particleboard	0	10.38 ± 0.91 ^{f}	0.95 ± 0.11^e	14.89	1.36	0.18 ± 0.07^c
	5	20.81 ± 1.03 ^{g}	2.87 ± 0.15 ^{f}	23.46	3.24	0.35 ± 0.10^c
	10	26.03 ± 1.22 ^{h}	3.34 ± 0.30 ^{g}	26.21	3.36	0.56 ± 0.11^c

the bonding between the fibers, as observed in the SEM images of the cross-section of broken fiberboards (Fig. 8). In the neat fiberboard, no adhesion between neighboring fibers was observed, and the fiber surfaces appeared clean. However, in the presence of LCNFs, an entangled network of cellulose fibrils was observed, likely originating from the LCNFs binder deposited on the fiber surfaces and creating bonds between different layers of fibers within the rapeseed fiberboard (Kojima et al., 2021).

One significant drawback of using fiber and particleboard in construction, apart from their susceptibility to water absorption and swelling, is their limited fire resistance. To assess their flammability, a commonly employed approach is the flammability test. Meeting the flammability standards set for commercial fiberboards is essential to demonstrate the technical viability of these materials for market use. Results of the flammability test are presented in Fig. 9, expressed as the required time by the flame to reach the 100 mm from the 25 mm mark, as detailed in the experimental section, as function of board density. Results are presented in these terms to further understand the effect of density and, thus, porosity, over the capacity of the flame to propagate through the lignocellulosic structure and how LCNFs can contribute to prevent its flammability.

The commercial fiberboard demonstrated a flame propagation time of 226 s to propagate from the first to the second mark. However, both the LCNF-free fiberboards and particleboards exhibited a shorter propagation time, indicating that these boards may not be suitable for the

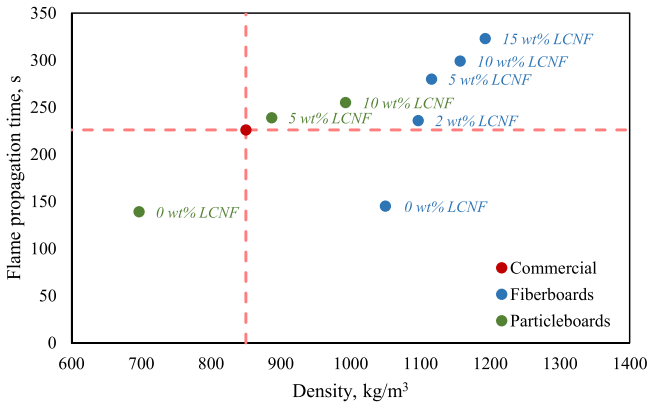

Fig. 9. Flame propagation time of commercial reference, fiberboards and particleboards as function of density. Dashed lines do not refer to data; they just indicate the position of the commercial reference data point.

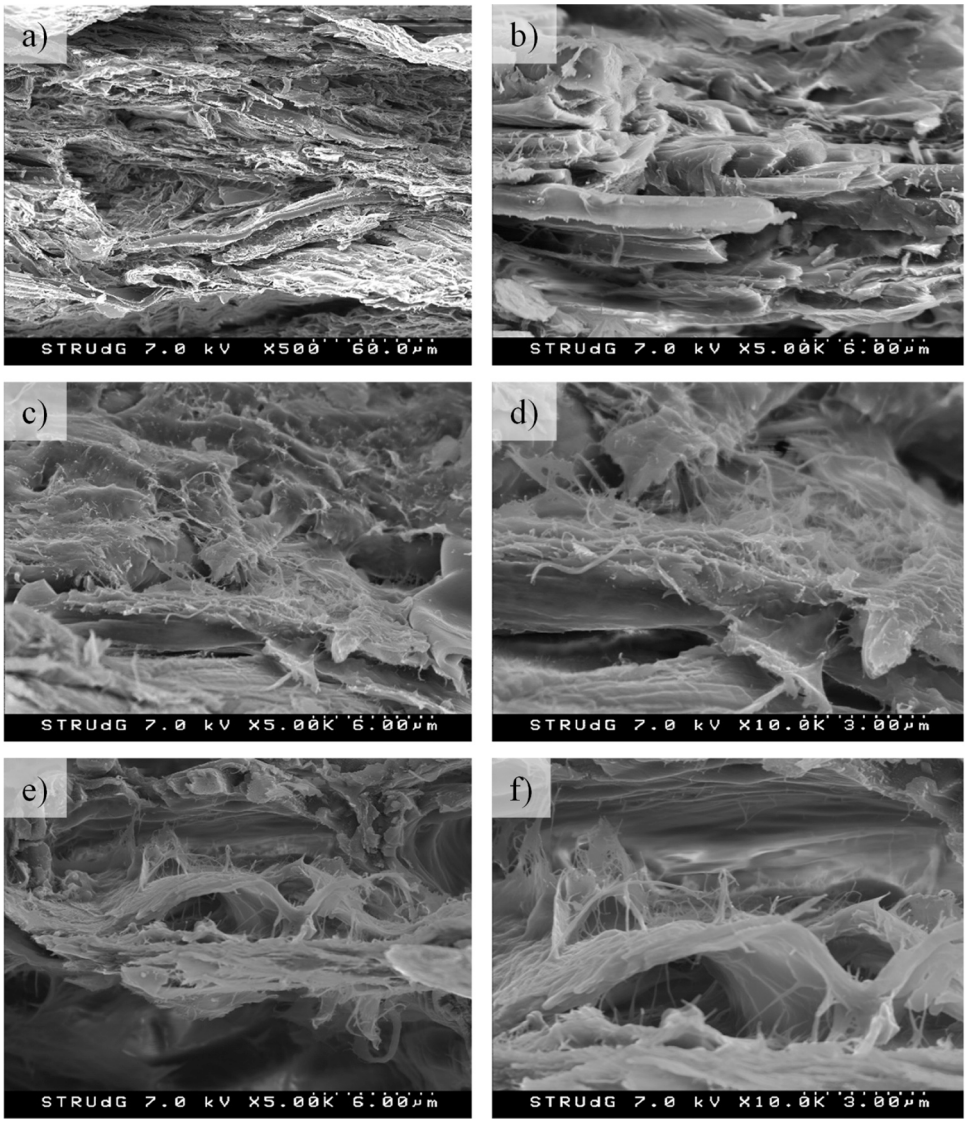

Fig. 8. SEM images of the cross section of the rapeseed fiberboards containing 0 wt% of LCNF (a, b), 5 wt% of LCNF (c, d), and 10 wt% of LCNF (e, f) at different magnification.

construction and building industry. It is important to consider the notable variations in density and, thus, porosity, as these factors can impact flame propagation (Bruce and Miniutti, 1957; Esmailpour et al., 2020). The inclusion of a 2 wt% LCNF in fiberboards and a 5 wt% LCNF in particleboards was sufficient to meet the flammability requirements of the commercial fiberboard. Furthermore, with an increase in LCNF content, the flame propagation time also increased. For example, the fiberboard reinforced with 15 wt% LCNF achieved a flame propagation time of 323 s. This suggests that density plays a significant role in limiting flame propagation. However, the relationship between density and flame spread is not always straightforward. For instance, the fiberboard without LCNFs (density of 1050 kg/m^3) and the particleboard with 10 wt% LCNFs (density of 993 kg/m^3) exhibited vastly different flame propagation times, despite their similar densities. The particleboard with LCNFs showed a 60% slower flame propagation compared to the fiberboard without LCNFs. This indicates that factors other than board compaction, such as the presence of LCNFs, may be inhibiting or hindering flame propagation. Moreover, the individualization of rapeseed fibers compared to particles did not significantly affect flame spread in materials without LCNFs. However, the addition of LCNFs can significantly impact flame propagation in these materials. Previous research by (Wang et al., 2020) showed that the inclusion of lignin in materials can enhance their resistance to fire. The formation of a carbon layer during lignin combustion acts as a barrier to the release of flammable gases, effectively retarding flame spread and combustion. The flame propagation can be observed in Video 1.

Supplementary material related to this article can be found online at doi:10.1016/j.indcrop.2023.117336.

4. Conclusions

The present work provides valuable insights into the binding capabilities of LCNFs as binders in the production of fiber and particle boards derived from agricultural residues. The findings clearly demonstrate a substantial decrease in the porosity of the fiberboards upon the addition of cellulose nanofibers, revealed by the increase on density. Although these effects were less pronounced in the particleboards due to the relatively lower binding capacity of the rapeseed particles, the incorporation of LCNF still contributed to the hydrophobization of the boards. This was evidenced by an increase in the contact angle formed by a droplet on the board surface. Remarkably, the addition of 15 wt% LCNF to produce a fiberboard resulted in a contact angle exceeding 90°, indicating a hydrophobic surface. Furthermore, the inclusion of LCNFs significantly enhanced moisture absorption and swelling properties, surpassing those of commercial fiberboards. Consequently, it can be confidently stated that LCNF-incorporated boards offer superior water resistance, making them suitable for applications in humid environments with improved performance compared to current boards.

Moreover, the mechanical properties of the boards were enhanced by the addition of LCNF, surpassing the performance of commercial boards, which initially exhibited superior properties. Specifically, the MOR, MOE, and IB of the boards achieved exceptional results when 15 wt% LCNF was added to rapeseed fibers.

Another significant contribution of LCNF was the enhancement of fire resistance in the boards. The results surpassed those of commercial boards, even with a LCNF content as low as 5 wt%. Therefore, it can be concluded that rapeseed fiberboards incorporating 15 wt% LCNF possess superior physical, mechanical, water resistance, and fire resistance properties compared to commercial boards. As a result, this material holds great promise for industrial implementation.

Overall, this research has demonstrated the remarkable potential of incorporating lignocellulosic nanofibers derived from date palm residues into rapeseed fiber and particle boards. The inclusion of LCNF significantly improved the binding capacity, reduced porosity, increased density, hydrophobized the surface, enhanced moisture absorption and swelling properties, improved mechanical strength, and increased fire resistance. These findings present a compelling case for the utilization of LCNF as a valuable component in the production of high-performance, sustainable boards for various industrial applications.

Funding information

This work has been funded by the Tunisian Ministry of Higher Education and Research, project 21P2ES-D6P3, and the Erasmus+ KA107 Program for the mobility grant of Amira Najahi.

CRediT authorship contribution statement

Amira Najahhi: Experimental. **Roberto J. Aguado:** Methodology, Writing – review & editing. **Quim Tarrés:** Conceptualization, Writing – original draft. **Sami Boufi:** Conceptualization, Writing – review & editing, Project administration, Funding acquisition. **Marc Delgado-Aguilar:** Conceptualization, Writing – review & editing, Project administration, Funding acquisition.

Declaration of Competing Interest

The authors declare the following financial interests/personal relationships which may be considered as potential competing interests: Dr. Sami Boufi reports financial support was provided by Tunisian Ministry of Higher Education and Research.

Data Availability

Data will be made available on request.

Acknowledgments

Authors wish to acknowledge the financial support of the funding agencies listed in the Funding section. Amira Najahi is grateful for the funding received by Erasmus for developing her internship at Universitat de Girona. Marc Delgado-Aguilar and Quim Tarrés are Serra Húnter Fellows.

Appendix A. Supporting information

Supplementary data associated with this article can be found in the online version at doi:10.1016/j.indcrop.2023.117336.

References

Aguilar, F.X., Mirzaee, A., McGarvey, R.G., Shifley, S.R., Burtraw, D., 2020. Expansion of US wood pellet industry points to positive trends but the need for continued monitoring. Sci. Rep. 10, 18607. https://doi.org/10.1038/s41598-020-75403-z.

Antov, P., Krišťák, L., Réh, R., Savov, V., Papadopoulos, A.N., 2021. Eco-friendly fiberboard panels from recycled fibers bonded with calcium lignosulfonate. Polymers 13, 1–14. https://doi.org/10.3390/polym13040639.

Arévalo, R., Peijs, T., 2016. Binderless all-cellulose fibreboard from microfibrillated lignocellulosic natural fibres. Compos Part A Appl. Sci. Manuf. 83, 38–46. https://doi.org/10.1016/j.compositesa.2015.11.027.

Bruce, H.D., Miniutti, V.P., 1957. Small tunnel furnace test for measuring surface flammability. Madison.

Buyle, M., Braet, J., Audenaert, A., 2013. Life cycle assessment in the construction sector: a review. Renew. Sustain. Energy Rev. https://doi.org/10.1016/j.rser.2013.05.001.

Candan, Z., Gardner, D.J., Shaler, S.M., 2016. Dynamic mechanical thermal analysis (DMTA) of cellulose nanofibril/nanoclay/pMDI nanocomposites. Compos B Eng. 90, 126–132. https://doi.org/10.1016/j.compositesb.2015.12.016.

Candan, Z., Tozluoglu, A., Gonultas, O., Yildirim, M., Fidan, H., Alma, M.H., Salan, T., 2022. Nanocellulose: Sustainable biomaterial for developing novel adhesives and composites. In: Sapuan, S.M., Norrahim, M.N.F. (Eds.), Industrial Applications of Nanocellulose and Its Nanocomposites. Woodhead Publishing, pp. 49–137.

Cheng, X., Zhu, S., Pan, Y., Deng, Y., Shi, L., Gong, L., 2020. Fire retardancy and thermal behaviors of Cellulose nanofiber/zinc borate aerogel. Cellulose 27, 7463–7474. https://doi.org/10.1007/s10570-020-03289-1.

Diop, C.I.K., Tajvidi, M., Bilodeau, M.A., Bousfield, D.W., Hunt, J.F., 2017. Evaluation of the incorporation of lignocellulose nanofibrils as sustainable adhesive replacement in medium density fiberboards. Ind. Crops Prod. 109, 27–36. https://doi.org/10.1016/j.indcrop.2017.08.004.

Domínguez-Robles, J., Tarrés, Q., Delgado-Aguilar, M., Rodríguez, A., Espinach, F.X., Mutjé, P., 2018. Approaching a new generation of fiberboards taking advantage of self lignin as green adhesive. Int. J. Biol. Macromol. 108. https://doi.org/10.1016/j.ijbiomac.2017.11.005.

Domínguez-Robles, J., Tarrés, Q., Alcalà, M., El Mansouri, N.-E., Rodríguez, A., Mutjé, P., Delgado-Aguilar, M., 2020. Development of high-performance binderless fiberboards from wheat straw residue. Constr. Build. Mater. 232. https://doi.org/10.1016/j.conbuildmat.2019.117247.

Dunky, M., Niemz, P., 2002. Wood Based Panels and Adhesive Resins: Technology and Influential Parameters. Springer, Heidelberg, pp. 1–986.

Esmailpour, A., Taghiyari, H.R., Ghorbanali, M., Mantanis, G.I., 2020. Improving fire retardancy of medium density fiberboard by nano-wollastonite. Fire Mater. 44, 759–766. https://doi.org/10.1002/fam.2855.

Fontes, A.M., Pirich, C.L., Tanobe, G.R.O.A., Tarrés, Q., Delgado-Aguilar, M., Ramos, L. P., 2021. Micro/nanostructured lignonanocellulose obtained from steam-exploded sugarcane bagasse. Cellulose 28, 10163–10182. https://doi.org/10.1007/s10570-021-04205-x.

Gan, V.J.L., Liu, T., Li, K., 2022. Integrated BIM and VR for interactive aerodynamic design and wind comfort analysis of modular buildings. Buildings 12. https://doi.org/10.3390/buildings12030333.

Halvarsson, S., Edlund, H., Norgren, M., 2009. Manufacture of non-resin wheat straw fibreboards. Ind. Crops Prod. 29, 437–445. https://doi.org/10.1016/j.indcrop.2008.08.007.

Hamawand, I., Seneweera, S., Kumarasinghe, P., Bundschuh, J., 2020. Nanoparticle technology for separation of cellulose, hemicellulose and lignin nanoparticles from lignocellulose biomass: a short review. Nano-Struct. Nano-Objects 24. https://doi.org/10.1016/j.nanoso.2020.100601.

Hashim, R., How, L.S., Kumar, R.N., Sulaiman, O., 2005. Some of the properties of flame retardant medium density fiberboard made from rubberwood and recycled containers containing aluminum trihydroxide. Bioresour. Technol. 96, 1826–1831. https://doi.org/10.1016/j.biortech.2005.01.023.

Hashim, R., Sulaiman, O., Kumar, R.N., Tamyez, P.F., Murphy, R.J., Ali, Z., 2009. Physical and mechanical properties of flame retardant urea formaldehyde medium density fiberboard. J. Mater. Process Technol. 209, 635–640. https://doi.org/10.1016/j.jmatprotec.2008.02.036.

Herrera, R., Erdocia, X., Llano-Ponte, R., Labidi, J., 2014. Characterization of hydrothermally treated wood in relation to changes on its chemical composition and physical properties. J. Anal. Appl. Pyrolysis 107, 256–266. https://doi.org/10.1016/j.jaap.2014.03.010.

Hýsek, Š., Gaff, M., Sikora, A., Babiak, M., 2018. New composite material based on winter rapeseed and his elasticity properties as a function of selected factors. Compos B Eng. 153, 108–116. https://doi.org/10.1016/j.compositesb.2018.07.042.

Ji, X., Li, B., Yuan, B., Guo, M., 2017. Preparation and characterizations of a chitosan-based medium-density fiberboard adhesive with high bonding strength and water resistance. Carbohydr. Polym. 176, 273–280. https://doi.org/10.1016/j.carbpol.2017.08.100.

Kaffashsaei, E., Yousefi, H., Nishino, T., Matsumoto, T., Mashkour, M., Madhoushi, M., 2023. Binderless self-densified 3 mm-thick board fully made from (Ligno)cellulose nanofibers of paulownia sawdust. Waste BiomassValoriz. https://doi.org/10.1007/s12649-023-02057-z.

Kim, K.-H., Jahan, S.A., Lee, J.-T., 2011. Exposure to formaldehyde and its potential human health hazards. J. Environ. Sci. Health Part C. 29, 277–299. https://doi.org/10.1080/10590501.2011.629972.

Kocaturk, E., Salan, T., Ozcelik, O., Alma, M.H., Candan, Z., 2023. Recent advances in lignin-based biofuel production. Energies. https://doi.org/10.3390/en16083382.

Kojima, Y., Kawabata, A., Kobori, H., Suzuki, S., Ito, H., Makise, R., Okamoto, M., 2016. Reinforcement of fiberboard containing lingo-cellulose nanofiber made from wood fibers. J. Wood Sci. 62, 518–525. https://doi.org/10.1007/s10086-016-1582-3.

Kojima, Y., Kato, N., Ota, K., Kobori, H., Suzuki, S., Aoki, K., Ito, H., 2019. Cellulose nanofiber as complete natural binder for particleboard. Prod. J. 68, 203–210. https://doi.org/10.13073/FPJ-D-18-00034.

Kojima, Y., Makino, T., Ota, K., Murayama, K., Kobori, H., Aoki, K., Suzuki, S., Ito, H., 2021. Evaluation of the mechanical and physical properties of insulation fiberboard with cellulose nanofibers. Prod. J. 71, 275–282. https://doi.org/10.13073/FPJ-D-21-00030.

Li, X., Li, Y., Zhong, Z., Wang, D., Ratto, J.A., Sheng, K., Sun, X.S., 2009. Mechanical and water soaking properties of medium density fiberboard with wood fiber and soybean protein adhesive. Bioresour. Technol. 100, 3556–3562. https://doi.org/10.1016/j.biortech.2009.02.048.

Li, Y., Chen, Y., Wu, Q., Huang, J., Zhao, Y., Li, Q., Wang, S., 2022. Improved hydrophobic, UV barrier and antibacterial properties of multifunctional PVA nanocomposite films reinforced with modified lignin contained cellulose nanofibers. Polymers 14. https://doi.org/10.3390/polym14091705.

Liu, X., Liu, Q., Wang, S., Liu, Z., Yang, G., Wang, H., Xiong, W., Li, P., Xu, F., Xi, Y., Kong, F., 2022. Effect of functional group and structure on hydrophobic properties of environment-friendly lignin-based composite coatings. Int. J. Biol. Macromol. 215, 132–140. https://doi.org/10.1016/j.ijbiomac.2022.06.055.

Mancera, C., Mansouri, N.-E., El, Vilaseca, F., Ferrando, F., Salvado, J., 2011. The effect of lignin as a natural adhesive on the physico-mechanical properties of Vitis vinifera fiberboards. Bioresources 6, 2851–2860.

Mancera, C., El Mansouri, N.-E., Pelach, M.A., Francesc, F., Salvadó, J., 2012. Feasibility of incorporating treated lignins in fiberboards made from agricultural waste. Waste Manag. 32, 1962–1967.

Mantanis, G.I., Martinka, J., Lykidis, C., Ševčík, L., 2020. Technological properties and fire performance of medium density fibreboard (MDF) treated with selected polyphosphate-based fire retardants. Wood Mater. Sci. Eng. 15, 303–311. https://doi.org/10.1080/17480272.2019.1596159.

Mazhari Mousavi, S.M., Hosseini, S.Z., Resalati, H., Mahdavi, S., Rasooly Garmaroody, E., 2013. Papermaking potential of rapeseed straw, a new agricultural-based fiber source. J. Clean. Prod. 52, 420–424. https://doi.org/10.1016/j.jclepro.2013.02.016.

Najahi, A., Tarrés, Q., Mutjé, P., Delgado-Aguilar, M., Putaux, J.L., Boufi, S., 2023. Lignin-containing cellulose nanofibrils from TEMPO-mediated oxidation of date palm waste: preparation, characterization, and reinforcing potential. Nanomaterials 13. https://doi.org/10.3390/nano13010126.

Nasir, M., Khali, D.P., Jawaid, M., Tahir, P.M., Siakeng, R., Asim, M., Khan, T.A., 2019. Recent development in binderless fiber-board fabrication from agricultural residues: a review. Constr. Build. Mater. 211, 502–516. https://doi.org/10.1016/j.conbuildmat.2019.03.279.

Nourbakhsh, A., Ashori, A., Jahan-Latibari, A., 2010. Evaluation of the physical and mechanical properties of medium density fiberboard made from old newsprint fibers. J. Reinf. Plast. Compos. 29, 5–11. https://doi.org/10.1177/0731684408093972.

Okuda, N., Hori, K., Sato, M., 2006. Chemical changes of kenaf core binderless boards during hot pressing (II): Effects on the binderless board properties. J. Wood Sci. 52, 249–254. https://doi.org/10.1007/s10086-005-0744-5.

Page, D.H., 1969. A theory for tensile strength of paper. Tappi 52, 674–681.

Rehman, Ur, Niaz, Z., Song, A.K., Il, J., Heun Koo, B., 2021. Excellent fire retardant properties of cnf/vmt based lbl coatings deposited on polypropylene and wood-ply. Polymers 13, 1–13. https://doi.org/10.3390/polym13020303.

Rojo, E., Peresin, M.S., Sampson, W.W., Hoeger, I.C., Vartiainen, J., Laine, J., Rojas, O.J., 2015. Comprehensive elucidation of the effect of residual lignin on the physical, barrier, mechanical and surface properties of nanocellulose films. Green. Chem. 17, 1853–1866. https://doi.org/10.1039/c4gc02398f.

Rowell, R.M., McSweeny, J.D., 2008. Heat treatments of wood fibers for self-bonding and stabilized fiberboards. Mol. Cryst. Liq. Cryst. 483, 307–325.

Schieweck, A., Uhde, E., Salthammer, T., Salthammer, L.C., Morawska, L., Mazaheri, M., Kumar, P., 2018. Smart homes and the control of indoor air quality. Renew. Sustain. Energy Rev. https://doi.org/10.1016/j.rser.2018.05.057.

Sehaqui, H., Allais, M., Zhou, Q., Berglund, L.A., 2011. Wood cellulose biocomposites with fibrous structures at micro- and nanoscale. Compos Sci. Technol. 71, 382–387. https://doi.org/10.1016/j.compscitech.2010.12.007.

Serra-Parareda, F., Aguado, R., Tarrés, Q., Mutjé, P., Delgado-Aguilar, M., 2021. Chemical-free production of lignocellulosic micro-and nanofibers from high-yield pulps: synergies, performance, and feasibility. J. Clean. Prod. 313, 127914.

Shinoda, R., Saito, T., Okita, Y., Isogai, A., 2012. Relationship between length and degree of polymerization of TEMPO-oxidized cellulose nanofibrils. Biomacromolecules 13, 842–849. https://doi.org/10.1021/bm2017542.

Shojaei, A., Ketabi, R., Razkenari, M., Hakim, H., Wang, J., 2021. Enabling a circular economy in the built environment sector through blockchain technology. J. Clean. Prod. 294 https://doi.org/10.1016/j.jclepro.2021.126352.

Sreejaya, M.M., Jeevan Sankar, R., K., R., Pillai, N.P., Ramkumar, K., Anuvinda, P., Meenakshi, V.S., Sadanandan, S., 2022. Lignin-based organic coatings and their applications: a review. Mater. Today Proc. 60, 494–501. https://doi.org/10.1016/j.matpr.2022.01.325.

Tarrés, Q., Saguer, E., Pèlach, M.A., Alcalà, M., Delgado-Aguilar, M., Mutjé, P., 2016. The feasibility of incorporating cellulose micro/nanofibers in papermaking processes: the relevance of enzymatic hydrolysis. Cellulose 1433–1445. https://doi.org/10.1007/s10570-016-0889-y.

Tarrés, Q., Boufi, S., Mutjé, P., Delgado-Aguilar, M., 2017. Enzymatically hydrolyzed and TEMPO-oxidized cellulose nanofibers for the production of nanopapers: morphological, optical, thermal and mechanical properties. Cellulose 24. https://doi.org/10.1007/s10570-017-1394-7.

Theng, D., Arbat, G., Delgado-Aguilar, M., Vilaseca, F., Ngo, B., Mutjé, P., 2015. All-lignocellulosic fiberboard from corn biomass and cellulose nanofibers. Ind. Crops Prod. 76, 166–173. https://doi.org/10.1016/j.indcrop.2015.06.046.

Theng, D., Arbat, G., Delgado-Aguilar, M., Ngo, B., Labonne, L., Evon, P., Mutjé, P., 2017. Comparison between two different pretreatment technologies of rice straw fibers prior to fiberboard manufacturing: twin-screw extrusion and digestion plus defibration. Ind. Crops Prod. 107, 184–197. https://doi.org/10.1016/j.indcrop.2017.05.049.

Theng, D., Arbat, G., Delgado-Aguilar, M., Ngo, B., Labonne, L., Mutjé, P., Evon, P., 2019. Production of fiberboard from rice straw thermomechanical extrudates by thermopressing: influence of fiber morphology, water and lignin content. Eur. J. Wood Wood Prod. 77, 15–32. https://doi.org/10.1007/s00107-018-1358-0.

Thomas, B., Raj, M.C., Athira, B.K., Rubiyah, H.M., Joy, J., Moores, A., Drisko, G.L., Sanchez, C., 2018. Nanocellulose, a versatile green platform: from biosources to materials and their applications. Chem. Rev. https://doi.org/10.1021/acs.chemrev.7b00627.

Tofanica, B.M., Cappelletto, E., Gavrilescu, D., Mueller, K., 2011. Properties of rapeseed (Brassica napus) stalks fibers. J. Nat. Fibers 8, 241–262. https://doi.org/10.1080/15440478.2011.626189.

Tozluoglu, A., Ates, S., Durmaz, E., Sertkaya, S., Arslan, R., Ozcelik, O., Candan, Z., 2022. Nanocellulose in paper and board coating. In: Taghiyari, H.R., Morrell, J.J., Husen, A. (Eds.), Emerging Nanomaterials. Springer, pp. 197–298.

Troilo, S., Besserer, A., Rose, C., Saker, S., Soufflet, L., Brosse, N., 2023. Urea-formaldehyde resin removal in medium-density fiberboards by steam explosion: developing nondestructive analytical tools. ACS Sustain Chem. Eng. 11, 3603–3610. https://doi.org/10.1021/acssuschemeng.2c05686.

Tsalagkas, D., Börcsök, Z., Pásztory, Z., Gryc, V., Csóka, L., Giagli, K., 2021. Agricultural residues content, BioResources.

Wang, Yuliang, Zhang, Y., Liu, Biying, Zhao, Q., Qi, Y., Wang, Yanmiao, Sun, Z., Liu, Baijun, Zhang, N., Hu, W., Xie, H., 2020. A novel phosphorus-containing lignin-based flame retardant and its application in polyurethane. Compos. Commun. 21 https://doi.org/10.1016/j.coco.2020.100382.

Xu, J., Han, G., Wong, E.D., Kawai, S., 2003. Development of binderless particleboard from kenaf core using steam-injection pressing. J. Wood Sci. 49, 327–332. https://doi.org/10.1007/s10086-002-0485-7.

Ye, X.P., Julson, J., Kuo, M., Womac, A., Myers, D., 2007. Properties of medium density fiberboards made from renewable biomass. Bioresour. Technol. 98, 1077–1084. https://doi.org/10.1016/j.biortech.2006.04.022.

Yildirim, M., Candan, Z., 2021. Particleboard with NC/BA. BioResources.

Yildirim, M., Candan, Z., Gonultas, O., 2021. Chemical performance analysis of nanocellulose/boron-compound-reinforced hybrid UF resin. Green. Mater. 10, 90–96. https://doi.org/10.1680/jgrma.20.00077.

Yildirim, M., Candan, Z., Aksoy, B., Dundar, T., 2022. Physico-mechanical properties and formaldehyde emission of plywood panels by lignosulfonate-reinforced urea-formaldehyde adhesive. Green. Mater. 1–10.

Zhang, D., Zhang, A., Xue, L., 2015. A review of preparation of binderless fiberboards and its self-bonding mechanism. Wood Sci. Technol. 49, 661–679. https://doi.org/10.1007/s00226-015-0728-6.

Zor, M., Mengeloglu, F., Aydemir, D., Sen, F., Kocatürk, E., Candan, Z., Ozcelik, O., 2022. Wood plastic composites (WPCs): applications of nanomaterials. In: Taghiyari, H.R., Morrell, J.J., Husen, A. (Eds.), Emerging Nanomaterials. Springer, pp. 97–133.